

Associating Imidazoles: Elucidating the Correlation between the Static Dielectric Permittivity and Proton Conductivity

Tyler Cosby, Zachariah Vicars, Maximilian Heres, and Joshua Sangoro*

Department of Chemical and Biomolecular Engineering, University of Tennessee, Knoxville, Tennessee 37996, USA



(Received 19 September 2017; revised manuscript received 30 January 2018; published 27 March 2018)

Broadband dielectric spectroscopy is employed to investigate the impact of supramolecular structure on charge transport and dynamics in hydrogen-bonded 2-ethyl-4-methylimidazole and 4-methylimidazole. Detailed analyses reveal (i) an inverse relationship between the average supramolecular chain length and proton conductivity and (ii) no direct correlation between the static dielectric permittivity and proton conductivity in imidazoles. These findings raise fundamental questions regarding the widespread notion that extended supramolecular hydrogen-bonded networks facilitate proton conduction in hydrogen bonding materials.

DOI: [10.1103/PhysRevLett.120.136001](https://doi.org/10.1103/PhysRevLett.120.136001)

Fundamental understanding of the dominant mechanisms of proton transport in amorphous hydrogen bonded materials is crucial for numerous applications ranging from proton exchange membranes to biological processes [1,2]. Proton conductivity in these systems is usually attributed either to vehicle and/or structure diffusion mechanisms. Structure diffusion is thought to involve fast proton transfer along supramolecular hydrogen-bonded networks via the Grotthuss mechanism, while vehicle diffusion is associated with transport of the protonated molecules whose rate limiting process is the primary structural relaxation. Computational studies have suggested that structure diffusion contributes significantly to proton conduction in certain amphoteric systems such as imidazoles, pyrazoles, benzimidazoles, triazoles, and phosphoric acid, especially due to the existence of extended supramolecular networks [3–6]. Therefore, these materials are at the forefront in the search for anhydrous proton exchange membranes with high proton conductivity, especially for applications in fuel cell technologies [1,7]. However, experimental evidence that extended supramolecular hydrogen-bonded structures actually facilitate proton conductivity through structure diffusion is limited and has, until now, relied on a comparison of charge and molecular diffusivities obtained by the Nernst-Einstein relation and ^1H NMR, respectively [8–10]. Furthermore, some authors have hypothesized that the high static dielectric permittivity (or dielectric constants) in these materials plays an important role in aiding charge dissociation and thereby increasing the effective number density of charge carriers, as is the case of other ion conducting materials [1,5,9,11]. The premise for this widespread notion is presumably Coulomb's law relating the static dielectric permittivity to the electrostatic force experienced by *point* charges. Concrete experimental evidence establishing the link between supramolecular

hydrogen-bonded networks, static dielectric permittivity, and proton transport in these materials is still lacking. Glass-forming imidazoles such as 2-ethyl-4-methylimidazole and, as we report here for the first time, 4-methylimidazole, exhibit a distinct slow Debye-like relaxation attributed to supramolecular chains and have the ability to dissociate under specific conditions, providing an ideal opportunity to probe the link between supramolecular hydrogen-bonded networks, dielectric constants, and proton transport. Results from these model systems will help in understanding proton conduction in similar supramolecular hydrogen-bonded materials.

A significant body of literature indicates that collective dynamics of supramolecular hydrogen-bonded networks gives rise to a slow, Debye-like relaxation in many hydrogen-bonding liquids such as monohydroxy alcohols, secondary amides, water, and 2-ethyl-4-methylimidazole [12–17]. The strengths of intermolecular interactions as well as the sizes and orientations of the supramolecular dipoles determine the effective dipole moment and the rate of the slow Debye-like relaxation, ω_{Debye} . Extensive studies of monohydroxy alcohols (MAs) have, for instance, revealed the existence of an equilibrium of ring-type and chain-type supramolecular hydrogen-bonded (H-bonded) structures, with the preferred orientations being sensitive to the molecular structure, pressure, and temperature [18–21]. Recent rheology and compressibility measurements on MAs revealed a terminal relaxation much slower than the primary structural relaxation, a response analogous to unentangled supramolecular polymers [22–26]. These studies suggest that the slow, Debye-like relaxation in the hydrogen bonded liquids originates from transient supramolecular chains which reorient by successive addition and removal of monomers at the chain ends. In this case, the Rouse model may be applied to describe the chain

dynamics and to provide quantitative estimates of the average sizes of the supramolecular structures. Although these studies enable quantitative estimates of the average lengths of supramolecular chains, MAs cannot easily dissociate due to their chemistry and are therefore not suitable candidates for understanding the correlation between supramolecular hydrogen bonded networks and proton conductivity.

In this study, we employ broadband dielectric spectroscopy to investigate the interplay between the static dielectric permittivity and proton conductivity in glass-forming 2-ethyl-4-methylimidazole and 4-methylimidazole. Detailed analysis of the dielectric data suggests preferential antiparallel alignment of chains comprising approximately seven imidazole molecules at all the temperatures probed. Further experiments using butyramide and levulinic acid as diluents—which either disrupt or preserve the supramolecular structures of 2-ethyl-4-methylimidazole—reveal that longer average chain lengths correlate with lower proton conductivity and higher static dielectric permittivity. These results challenge the longstanding notion that higher static dielectric permittivity in this class of supramolecular hydrogen bonded materials results in enhanced proton conduction. This apparent disparity is attributed to the fact that proton transport in these materials is controlled by the primary structural dynamics while the static dielectric permittivity arises from the additivity of dipole moments comprising the supramolecular chains characterized by dynamics at much longer timescales.

Broadband dielectric spectroscopy is a versatile experimental tool for investigating the dynamics of dipolar and ionic materials [27]. Application of an oscillating electric field of small amplitude to these materials over a broad temperature range enables one to probe the dynamics of polar molecular and supramolecular moieties as well as charge transport. The dielectric spectra of the associating imidazoles reveal two relaxations as evident in the real part of complex dielectric permittivity, ϵ' , and its corresponding derivative loss spectra, ϵ''_{der} , for 2-ethyl-4-methylimidazole (2E4MIm) (Fig. 1). The derivative representation is employed since it suppresses the contributions of proton conductivity to the dielectric loss while revealing the underlying dielectric relaxations. The solid lines in Fig. 1 represent fits obtained by a linear combination of two Havriliak-Negami functions. The faster dielectric process corresponds to the primary structural, α -relaxation of the 2E4MIm molecules and the slower, Debye-like relaxation is attributed to reorientation of supramolecular hydrogen-bonded chains [28,29]. The low frequency static dielectric permittivity values, indicated in Fig. 1(a), show a minimum at 280 K owing to a strong temperature dependence of the dielectric relaxation strength $\Delta\epsilon_{\text{Debye}}$. The static dielectric permittivity of associated liquids reflects the supramolecular networks inherent in these materials especially if such networks serve to preferentially orient neighboring dipolar moieties either parallel or antiparallel to one another. The departure from the

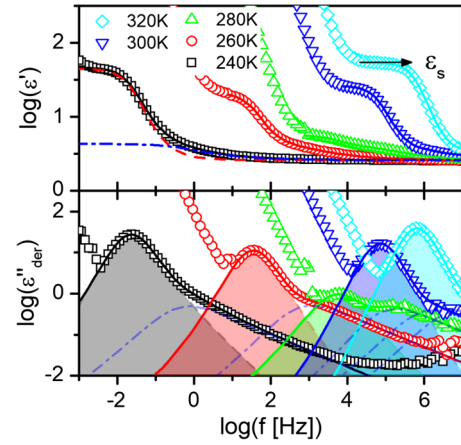


FIG. 1. Broadband dielectric spectra of 2-ethyl-4-methylimidazole. Real part of the complex dielectric function ϵ' and the derivative spectra $\epsilon''_{\text{der}} = [(-\pi)/2]\{(\partial\epsilon')/[\partial\ln(f)]\}$ of pure 2-ethyl-4-methylimidazole (2E4MIm) vs frequency. Solid lines represent fits using a combination of two Havriliak-Negami fitting functions. Shaded areas depict the contribution of the slow, Debye-like relaxation and dotted-dashed blue lines correspond to the structural α relaxation.

Onsager relation—which describes the static dielectric permittivity of non-associated dipolar liquids—due to the orientation as described by the Kirkwood-Fröhlich correlation factor, g_K , is quantified by the expression $\epsilon_s - \epsilon_\infty = [(3\epsilon_s)/(2\epsilon_s + \epsilon_\infty)][(\epsilon_\infty + 2)/3]^2[(N\mu^2)/(3kT)]g_K$, where ϵ_s is the static dielectric permittivity, ϵ_∞ the real part of permittivity in the high frequency limit, N the number density of dipoles, and μ the dipole moment [30]. Values of g_K above or below 1 indicate a preference for parallel or antiparallel orientation of neighboring dipoles, respectively [30]. The dielectric strength of $\Delta\epsilon_\alpha$ is lower than expected. The suppression of $\Delta\epsilon_\alpha$ has also been observed in monohydroxy alcohols and water and is attributed to a reduction in the degrees of freedom available to the molecule at the timescale of the α relaxation [17,18,31].

The static dielectric permittivity, $\epsilon_s = \Delta\epsilon_{\text{Debye}} + \Delta\epsilon_\alpha + \epsilon_\infty$, of 2-ethyl-4-methylimidazole and 4-methylimidazole is given as a function of temperature in Fig. 2 (closed symbols) alongside the corresponding g_K (lines), revealing competing parallel and antiparallel orientations of neighboring imidazole dipoles. In monohydroxy alcohols, such a temperature dependence of static permittivity is associated with a shifting orientation of the relaxing supramolecular structures, as first suggested by Dannhauser in the 1960s [12,13]. As temperature is decreased, ring-type supramolecular structures begin to form followed by a transition to predominantly linear chains at the lowest temperatures. The transition from rings to chains would geometrically require lengthening of the supramolecular structures and therefore a concomitant decrease in ω_{Debye} with respect to ω_α has been observed in all MAs showing this type of temperature dependent static dielectric permittivity. The decrease in values of ω_{Debye} has

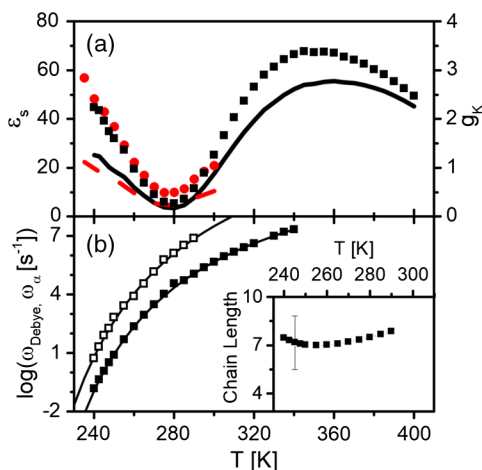


FIG. 2. (a) Static dielectric permittivity ϵ_s of pure 2-ethyl-4-methylimidazole (2E4MIm, closed squares) and 4-methylimidazole (4MIm, closed circles). The departure from the Onsager relation is captured by the Kirkwood correlation factor, g_k (solid and dashed lines corresponding to 2E4MIm and 4MIm, respectively). (b) Relaxation rates of the structural, α relaxation (open squares) and slow, Debye-like relaxation (closed squares) of 2E4MIm. Solid lines represent fits by the Vogel-Fulcher-Tammann equation, $\omega = \omega_{\infty} \exp[B/(T - T_0)]$, see Supplemental Material [37]. Inset: Estimated number of molecules participating in a chain, chain length $\approx (\omega_{\alpha}/\omega_{\text{Debye}})^{1/2}$.

been confirmed by dielectric and shear-mechanical spectroscopy as well as compressibility measurements [18,26,32–36]. However, in the case of 2E4MIm the ratio between ω_{Debye} and ω_{α} remains approximately constant over the entire temperature range in which g_k transitions from above to below 1, suggesting that the average lengths of the supramolecular structures remain relatively unaltered in the entire range.

Evidence of the formation of a variety of linear oligomers in imidazoles has been reported from solution infrared studies; however, the formation of cyclic oligomers with less than 10 repeat molecules would result in strained hydrogen bonds and are therefore highly unlikely [45]. The transient chain mechanism, which describes the slow, Debye-like relaxation of MAs, provides an avenue to estimate an average length of supramolecular chains by applying models developed to describe polymer dynamics [24,31,56–58]. The Rouse model, which describes the dynamics of short chain polymers, reveals a temperature-independent average chain length, $n \approx \sqrt{\omega_{\alpha}/\omega_{\text{Debye}}}$, of approximately *seven* 2-ethyl-4-methylimidazole molecules [inset of Fig. 2(b)]. Therefore, if the depression in static permittivity vs temperature were due to a shift in the equilibrium of chain and ring structures, the average lengths of the structures would need to drastically increase as temperature is decreased. However, the ratio $\omega_{\alpha}/\omega_{\text{Debye}}$ is temperature independent over the range 240–290 K (Fig. 2), indicating that the average length of the chains

remains unaltered. Furthermore, the slow Debye-like relaxation in 2E4MIm has been observed up to 450 K by Brillouin-Raman spectroscopy with negligible reduction in the ratio $\omega_{\alpha}/\omega_{\text{Debye}}$ [28]. Therefore, we suggest that the antiparallel orientation of 2E4MIm originates not from ring formation, but from an increase in the preference for antiparallel alignment of linear chains. While the precise reason for the change in preferred alignment cannot be conclusively determined from the current results, we conjecture that the ability of imidazole molecules to engage in $\pi - \pi$ interactions is a contributing factor to this mechanism. Further experimental and computational work, out of the scope of the current work, are required to unravel the role of $\pi - \pi$ interactions in determining supramolecular hydrogen bonding in this class of materials.

Further insight into the influence of supramolecular structure on the charge transport and dynamics of 2E4MIm is provided by examining the influence of additives on the average lengths of the supramolecular structures, the dielectric strength of the slow, Debye-like relaxation, and the measured proton conductivity. In a previous work, we proposed that the supramolecular chains of 2-ethyl-4-methylimidazole are disrupted by addition of 2.5 mol % levulinic acid (LA) as indicated by shifts in the rates obtained by dynamic light scattering and broadband dielectric spectroscopy as well as a reduction in the viscosity [29]. An inspection of the dielectric spectra over a broader acid concentration range reveals a gradual increase in ω_{Debye} , attributed to a shortening of the average chain lengths, Fig. 3(a). Because of the decreasing separation between ω_{α} and ω_{Debye} , the dielectric spectra of the acid mixtures are fit with a combination of one Havriliak-Negami function, to account for the slow, Debye-like relaxation, and the random barrier model (RBM), to

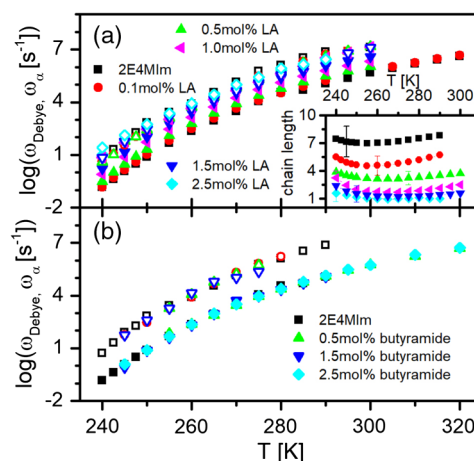


FIG. 3. Relaxation rate vs temperature for the slow, Debye-like relaxation (closed symbols) and structural, α relaxation (open symbols) of pure 2-ethyl-4-methylimidazole and low concentration (a) levulinic acid and (b) butyramide mixtures as obtained from the broadband dielectric spectra.

account for the faster charge hopping process. The structural, α -relaxation rate of pure 2E4MIm corresponds with the charge hopping rate obtained by the RBM as seen in Fig. 3. The dielectric spectra as well as details of the fitting equations are provided in the Supplemental Material [37]. Based on the separation of the two relaxation rates, it is apparent that the extended supramolecular hydrogen-bonded chains are disrupted at and above 1.5 mol % LA. The disruption in supramolecular structure is sensitive to the type of diluent and appears to rely on its ability to donate protons as shown by the invariance of relaxation rates upon addition of nonproton donating butyramide, Fig. 3(b).

The loss of linear hydrogen-bonded structures upon addition of levulinic acid is expected to reduce the parallel correlations of neighboring dipoles. That is, it will decrease the static dielectric permittivity in the regime where $g_K > 1$. Because of the unknown influence of the shortening of hydrogen-bonded chains on the interplay between parallel and antiparallel orientations of neighboring dipoles, the actual influence of acid addition on ϵ_s is not so straightforward, as seen in Fig. 4(a). Despite this, two observations may still be made: (i) values where $g_K < 1$ continue to be observed up to 2.5 mol % LA and (ii) the values and temperature dependence of ϵ_s approach the prediction of Onsager's relation for pure 2E4MIm at 10 mol % LA. The observation of antiparallel orientation at concentrations where the chains are significantly shorter is a strong indication that such orientation does not originate in ring-type supramolecular structures. The continued departure from Onsager's relation up to approximately 10 mol % LA indicates a contribution from linearly H-bonded structures. This interpretation of the dielectric spectra is qualitatively supported by Fourier-transform infrared spectroscopy measurements of 2E4MIm and the levulinic acid mixtures. The "association" band centered at

1880 cm^{-1} in pure 2E4MIm is blueshifted by approximately 80 cm^{-1} as the acid concentration is increased from 0–20 mol % LA, indicating a perturbation of the hydrogen bonding network; see the Supplemental Material [37]. A significant increase in the ionic conductivity accompanies the disruption of the extended supramolecular chains, see Fig. 5. Fast proton transport by structure diffusion mechanism should be strongly hindered by the reduction in the average lengths of the extended hydrogen-bonded structures [59]. In contrast, it is observed that the ionic conductivity is enhanced at all acid concentrations measured. The increase may be attributed to an increase in the effective number density of mobile charge carriers.

The constant average chain length upon addition of the hydrogen bonding, but nonproton donating butyramide molecule is illuminating. The static dielectric permittivity, by comparison, is significantly influenced upon addition of butyramide, Fig. 4(b). The minimum shifts to lower temperatures while the value at the maximum increases from 68 to 88. The shift in ϵ_s is due to changes in dielectric strength of the slow, Debye-like relaxation, $\Delta\epsilon_{\text{Debye}}$, see Supplemental Material [37]. Alongside the continued presence of the minimum in ϵ_s at lower temperatures this suggests that the increase may still be assigned to the dominant contribution of the supramolecular structures in 2E4MIm. However, the butyramide molecules also contribute to the measured ϵ_s as well due to their high dipole moments even though their concentration is low. It is worth noting that a similar effect is observed when one compares the magnitude of the static dielectric permittivity for neat 2E4MIm of different purities of 95% and 99%, reported in the previous studies [28,29]. In both cases, slightly shifted minima in the plot of the ϵ_s vs temperature are observed, but the characteristic timescales remain unaltered. It should

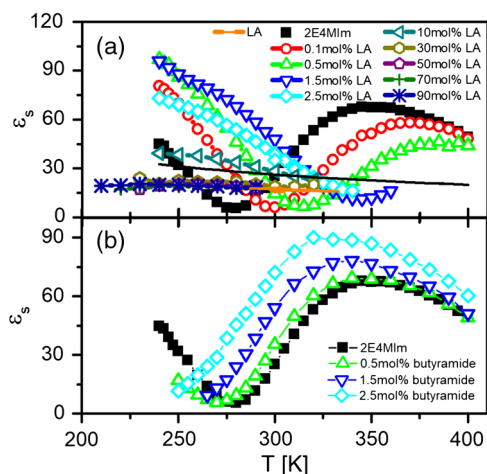


FIG. 4. Static dielectric permittivity vs temperature of 2-ethyl-4-methylimidazole and its mixtures with (a) levulinic acid and (b) butyramide. Solid line is the static permittivity predicted for pure 2E4MIm by the Onsager relation.

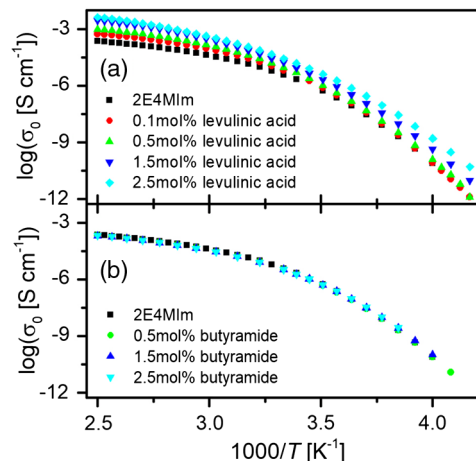


FIG. 5. Ionic conductivity σ_0 as a function of inverse temperature for (a) levulinic acid and (b) butyramide mixtures with 2-ethyl-4-methylimidazole. Minute amounts of levulinic acid substantially increase the ionic conductivity, while butyramide has no effect.

be noted that in previous studies of 2-ethyl-4-methylimidazole, no analysis and discussion of the temperature dependence of ϵ_s was provided [28]. Therefore, any direct correlation between the average length of the supramolecular chains and the static dielectric permittivity as well as proton conductivity could not be established. In addition, although we conjectured that addition of levulinic acid to 2-ethyl-4-methylimidazole leads to disruption of the supramolecular hydrogen-bonded chains, this hypothesis could not be confirmed since much higher concentrations (≥ 2.5 mol%) of the acid were used in the previous study [29].

In addition to the new insights obtained from the present study regarding the interplay between the static dielectric permittivity and proton transport, the use of suitable diluents makes it possible to verify the previous hypothesis regarding the shortening of the supramolecular chains upon addition of levulinic acid. The measured ionic conductivity σ_0 shows no change over the same butyramide concentrations. Because of the strongly temperature dependent static dielectric permittivity of neat 2E4MI and the absence of a direct correlation between static dielectric permittivity with ionic conductivity in the butyramide mixtures, we conclude that the static dielectric permittivity in imidazoles with slow, sub- α relaxation dynamics is not directly linked to proton conductivity, in contrast to prevailing opinion in the current scientific literature [1,5,6,11]. We attribute this apparent discrepancy to the fact that proton transport in these materials is controlled by the structural α relaxation while the static dielectric permittivity arises from the vector addition of the dipole moments comprising the supramolecular chains, for which the characteristic timescales of dynamics are much slower.

In summary, we have reported a strong nonmonotonic temperature dependence of the static dielectric permittivity in glass-forming 4-methylimidazole and 2-ethyl-4-methylimidazole. Deviations from the Onsager relation indicate preferential antiparallel alignment of neighboring imidazole molecules. Using the Rouse model, it is found that the supramolecular chains in neat 2-ethyl-4-methylimidazole consist of approximately seven imidazole molecules at all the temperatures probed. Further experiments using butyramide and levulinic acid as diluents reveal that longer average chain lengths of the supramolecular chains correlate with lower proton conductivity and higher static dielectric permittivity. These results challenge the long-standing notion that higher static dielectric permittivity (or constant) in this class of supramolecular hydrogen bonded materials enhances proton conduction. The apparent disparity is attributed to the fact that proton transport in these materials is determined by the primary structural dynamics while the static dielectric permittivity arises from the additivity of dipole moments comprising the supramolecular chains with dynamics at much longer characteristic timescales.

Z. V. and J. S. acknowledge support by the National Science Foundation, the Division of Materials Research, Polymers Program through Grant No. DMR-1508394. T. C. gratefully acknowledges financial support from the U.S. Army Research Office under Contract No. W911NF-17-1-0052. In addition, the authors thank Austen Angell, Roberto Benson, and Emmanuel Mapesa for helpful comments and suggestions about the work. The temperature dependent infrared spectroscopy measurements were conducted at the Oak Ridge National Laboratory's Center for Nanophase Materials Sciences, which is sponsored by the Division of Scientific User Facilities, Office of Basic Energy Sciences, U.S. Department of Energy.

*jsangoro@utk.edu

- [1] K.-D. Kreuer, S. J. Paddison, E. Spohr, and M. Schuster, *Chem. Rev.* **104**, 4637 (2004).
- [2] J. T. Daycock, G. P. Jones, J. R. N. Evans, and J. M. Thomas, *Nature (London)* **218**, 672 (1968).
- [3] S. Scheiner and M. Y. Yi, *J. Phys. Chem.* **100**, 9235 (1996).
- [4] I. Fischbach, H. W. Spiess, K. Saalwachter, and G. R. Goward, *J. Phys. Chem. B* **108**, 18500 (2004).
- [5] H. Steininger, M. Schuster, K. D. Kreuer, A. Kaltbeitzel, B. Bingöl, W. H. Meyer, S. Schauff, G. Brunklus, J. Maier, and H. W. Spiess *Phys. Chem. Chem. Phys.* **9**, 1764 (2007).
- [6] W. Bua-ngern, S. Chaiwongwattana, P. Suwannakham, and K. Sagarik, *RSC Adv.* **6**, 99391 (2016).
- [7] Y. B. Chen, M. Thorn, S. Christensen, C. Versek, A. Poe, R. C. Hayward, M. T. Tuominen, and S. Thayumanavan, *Nat. Chem.* **2**, 503 (2010).
- [8] K. D. Kreuer, A. Fuchs, M. Ise, M. Spaeth, and J. Maier, *Electrochim. Acta* **43**, 1281 (1998).
- [9] W. Munch, K. D. Kreuer, W. Silvestri, J. Maier, and G. Seifert, *Solid State Ionics* **145**, 437 (2001).
- [10] T. Yasuda and M. Watanabe, *MRS Bull.* **38**, 560 (2013).
- [11] J. Thisuwan and K. Sagarik, *RSC Adv.* **4**, 61992 (2014).
- [12] W. Dannhauser, *J. Chem. Phys.* **48**, 1911 (1968).
- [13] G. P. Johari and W. Dannhauser, *J. Chem. Phys.* **48**, 5114 (1968).
- [14] M. A. Floriano and C. A. Angell, *J. Chem. Phys.* **91**, 2537 (1989).
- [15] L. M. Wang and R. Richert, *J. Phys. Chem. B* **109**, 11091 (2005).
- [16] R. Böhmer, C. Gainaru, and R. Richert, *Phys. Rep.* **545**, 125 (2014).
- [17] J. S. Hansen, A. Kisliuk, A. P. Sokolov, and C. Gainaru, *Phys. Rev. Lett.* **116**, 237601 (2016).
- [18] L. P. Singh and R. Richert, *Phys. Rev. Lett.* **109**, 167802 (2012).
- [19] C. Gainaru, M. Wikarek, S. Pawlus, M. Paluch, R. Figuli, M. Wilhelm, T. Hecksher, B. Jakobsen, J. C. Dyre, and R. Böhmer, *Colloid Polym. Sci.* **292**, 1913 (2014).
- [20] D. Fragiadakis, C. M. Roland, and R. Casalini, *J. Chem. Phys.* **132**, 144505 (2010).
- [21] K. Adrjanowicz, B. Jakobsen, T. Hecksher, K. Kaminski, M. Dulski, M. Paluch, and K. Niss, *J. Chem. Phys.* **143**, 181102 (2015).

- [22] B. Jakobsen, C. Maggi, T. Christensen, and J. C. Dyre, *J. Chem. Phys.* **129**, 184502 (2008).
- [23] T. Hecksher and B. Jakobsen, *J. Chem. Phys.* **141**, 101104 (2014).
- [24] C. Gainaru, R. Figuli, T. Hecksher, B. Jakobsen, J. C. Dyre, M. Wilhelm, and R. Böhmer, *Phys. Rev. Lett.* **112**, 098301 (2014).
- [25] S. Bauer, K. Moch, P. Munzner, S. Schildmann, C. Gainaru, and R. Bohmer, *J. Non-Cryst. Solids* **407**, 384 (2015).
- [26] T. Hecksher, *J. Chem. Phys.* **144**, 161103 (2016).
- [27] F. Kremer and A. Schönhal, *Broadband Dielectric Spectroscopy* (Springer-Verlag, Berlin, 2003).
- [28] Y. Wang, P. J. Griffin, A. Holt, F. Fan, and A. P. Sokolov, *J. Chem. Phys.* **140**, 104510 (2014).
- [29] T. Cosby, A. Holt, P. J. Griffin, Y. Y. Wang, and J. Sangoro, *J. Phys. Chem. Lett.* **6**, 3961 (2015).
- [30] H. Fröhlich, *Theory of Dielectrics* (Clarendon, Oxford, 1958).
- [31] C. Gainaru, R. Meier, S. Schildmann, C. Lederle, W. Hiller, E. A. Rossler, and R. Bohmer, *Phys. Rev. Lett.* **105**, 258303 (2010).
- [32] T. Hecksher and B. Jakobsen, *J. Chem. Phys.* **141**, 101104 (2014).
- [33] S. Bauer, K. Burlafinger, C. Gainaru, P. Lunkenheimer, W. Hiller, A. Loidl, and R. Bohmer, *J. Chem. Phys.* **138**, 094505 (2013).
- [34] S. Bauer, H. Wittkamp, S. Schildmann, M. Frey, W. Hiller, T. Hecksher, N. B. Olsen, C. Gainaru, and R. Bohmer, *J. Chem. Phys.* **139**, 134503 (2013).
- [35] L. P. Singh, A. Raihane, C. Alba-Simionesco, and R. Richert, *J. Chem. Phys.* **142**, 014501 (2015).
- [36] L. P. Singh, C. Alba-Simionesco, and R. Richert, *J. Chem. Phys.* **139**, 144503 (2013).
- [37] See Supplemental Material at <http://link.aps.org/supplemental/10.1103/PhysRevLett.120.136001> for sample preparation, experimental techniques, details on fitting of dielectric data, dielectric spectra of mixtures, calculation of g_k , and FTIR spectra, which includes Refs. [38–55].
- [38] A. R. Katritzky, C. A. Ramsden, J. A. Joule, and V. V. Zhadankin, *Handbook of Heterocyclic Chemistry*, 3rd ed. (Elsevier, Amsterdam, 2010).
- [39] M. L. Jimenez, F. J. Arroyo, J. van Turnhout, and A. V. Delgado, *J. Colloid Interface Sci.* **249**, 327 (2002).
- [40] H. Wolff and H. Müller, *J. Chem. Phys.* **60**, 2938 (1974).
- [41] A. B. McCoy, *J. Phys. Chem. B* **118**, 8286 (2014).
- [42] P. K. Verma, A. Kundu, M. S. Poretz, C. Dhoonmoon, O. S. Chegwidan, C. H. Londergan, and M. Cho, *J. Phys. Chem. B* **122**, 2587 (2018).
- [43] S. Giuffrida, G. Cottone, and L. Cordone, *Phys. Chem. Chem. Phys.* **19**, 4251 (2017).
- [44] D. Eisenberg and W. Kauzmann, *The Structure and Properties of Water* (Oxford University Press, New York, 1969).
- [45] D. M. Anderson, J. L. Duncan, and F. J. Rossotti, *J. Chem. Soc.* **140**, 2165 (1961).
- [46] C. Perchard and A. Novak, *J. Chem. Phys.* **48**, 3079 (1968).
- [47] D. H. Bonsor, B. B. Borah, R. L. Dean, and J. L. Wood, *Can. J. Chem.* **54**, 2458 (1975).
- [48] W. Tataru, M. Wojcik, J. Lindgrin, and M. Probst, *J. Phys. Chem. A* **107**, 7827 (2003).
- [49] M. J. Wójcik, J. Kwiendacz, M. Boczar, Ł. Boda, and Y. Ozaki, *Chem. Phys.* **372**, 72 (2010).
- [50] K. Hasegawa, T. Ono, and T. Noguchi, *J. Phys. Chem. B* **104**, 4253 (2000).
- [51] M. Majoube, P. Millie, and G. Vergoten, *J. Mol. Struct.* **344**, 21 (1995).
- [52] F. Billes, H. Endrédi, and G. Jalsovszky, *J. Mol. Struct. THEOCHEM* **465**, 157 (1999).
- [53] S. Lee, S. Jun Lee, A. Ahn, Y. Kim, A. Min, M. Yong Choi, and R. E. Miller, *Bull. Korean Chem. Soc.* **32**, 885 (2011).
- [54] A.-M. Bellocq and C. Garrigou-Lagrange, *Spectrochim. Acta, Part A* **27**, 1091 (1971).
- [55] S. Giuffrida, G. Cottone, F. Librizzi, and L. Cordone, *J. Phys. Chem. B* **107**, 13211 (2003).
- [56] S. Arrese-Igor, A. Alegría, and J. Colmenero, *J. Chem. Phys.* **142**, 214504 (2015).
- [57] S. Arrese-Igor, A. Alegría, and J. Colmenero, *J. Chem. Phys.* **146**, 114502 (2017).
- [58] M. Monkenbusch, M. Krutyeva, W. Pyckhout-Hintzen, W. Antonius, C. H. Hövelmann, J. Allgaier, A. Brás, B. Farago, A. Wischnewski, and D. Richter, *Phys. Rev. Lett.* **117**, 147802 (2016).
- [59] R. A. Munson and M. E. Lazarus, *J. Phys. Chem.* **71**, 3245 (1967).